

Behaviour of a polar relaxation mode around the phase transition point in the antiferroelectric PbZrO_3 single crystal

This article has been downloaded from IOPscience. Please scroll down to see the full text article.

1996 J. Phys.: Condens. Matter 8 10669

(<http://iopscience.iop.org/0953-8984/8/49/051>)

View [the table of contents for this issue](#), or go to the [journal homepage](#) for more

Download details:

IP Address: 171.66.16.207

The article was downloaded on 14/05/2010 at 05:52

Please note that [terms and conditions apply](#).

Behaviour of a polar relaxation mode around the phase transition point in the antiferroelectric PbZrO_3 single crystal

K Roleder[†], M Maglione[‡], M D Fontana[§] and J Dec[†]

[†] Institute of Physics, University of Silesia, 40007 Katowice, Poland

[‡] Laboratoire de Physique, University of Bourgogne, 21004 Dijon, France

[§] Laboratoire Matériaux Optiques a Propriétés Spécifiques, Centre Lorrain d'Optique et Electronique des Solides, University of Metz and Supelec, 57078 Metz Cédex 3, France

Received 10 July 1996

Abstract. In measurements of the dielectric dispersion carried out on single crystals of antiferroelectric lead zirconate (PbZrO_3) a polar relaxation mode in the frequency range from 10^6 to 10^9 Hz has been found. Using the Cole–Cole relation for the complex $\varepsilon(\omega)$ response the relaxation frequency and dielectric step of the mode have been determined as functions of temperature. In the paraelectric phase the squared relaxation frequency well obeys a relation $f_r^2 \sim (T - T_0)$ with $T_0 = 222.9^\circ\text{C}$. The temperature dependence of the dielectric step corresponds to a sharp anomaly of the dielectric permittivity observed at the phase transition between the paraelectric and antiferroelectric states in PbZrO_3 . The phase transition mechanism of order–disorder type is discussed considering a disorder of the Pb sublattice in the paraelectric phase.

It should be pointed out that similar dipolar relaxation in ABO_3 perovskites is known to appear only in those with ferroelectric properties.

1. Introduction

The high-symmetry ABO_3 perovskite structure in the paraelectric phase ($Pm3m$) is simple cubic with oxygen atoms at the face centres and metals A and B at the cube corner and body centre, respectively. In this structure, two instabilities, i.e. ferroelectric and antiferroelectric instabilities, result from a softening of either a zone-centre polar phonon mode (Γ_{15}) or a non-polar zone-boundary mode involving rigid rotations of oxygen octahedra (Γ_{25}) [1]. Among the ABO_3 perovskites, PbZrO_3 has a strong antiferroelectric instability although the ferroelectric instabilities were also predicted [1, 2]. This is consistent with an earlier analysis by Cochran and Zia [3] indicating that the antiferroelectric room-temperature structure of lead zirconate is made up of mode displacements of Γ_{15} , Γ_{25} , Σ_3 and M_5 . In neutron diffraction carried out by Fujishita and Hoshino [4] the structure was found to be described by a sum of modulations associated with the lattice vibrational modes Σ_3 , R_{25}^x and R_{25}^y . Theoretical investigations using local-density calculations [5] showed that the ground state of antiferroelectric nature is favoured provided that oxygen ions can take independent coordinates. Of several papers on the structural properties of lead zirconate, a review of which can be found in [6], neutron diffraction [4] supports those theoretical predictions on oxygen positions. In all structural studies it was assumed that the structure was fully ordered. It should be mentioned that there are still some controversies in determining the

antiferroelectric structure of lead zirconate which probably might be connected with the type of material (ceramic or crystal) and the stoichiometry of samples used.

Although a large anomaly in the dielectric permittivity at T_c was clearly detected, no soft-mode behaviour has yet been reported for PbZrO_3 . Raman light scattering in this crystal [7, 8] showed some anomalies at phase transitions but did not reveal a clear low-frequency mode softening below T_c . Only a peak detected at room temperature around 130 cm^{-1} shifts very slowly with temperature towards lower frequencies, being strongly overdamped when approaching the phase transition point. Regardless of the fact that the frequency of this line corresponds to that theoretically calculated and considered as the soft-mode frequency in PbZrO_3 [2] its softening seems to be insufficient to account for the value of the ε' peak at T_c .

In the case of the ferroelectric perovskites such as barium titanate, potassium niobate and lead titanate the soft-mode concept does not fully explain the $\varepsilon'(T)$ function, and relaxational dynamics of Ti/Nb inside the oxygen octahedra (BaTiO_3 or KNbO_3) or Pb and O about their displaced sites (PbTiO_3) were postulated to be responsible for the dielectric response measured in the radio-frequency range [9–12]. In all cases a crossover between the displacive and order–disorder mechanism of transformation near T_c was thus discussed. In ceramic lead zirconate a dielectric relaxation at a microwave frequency was reported by Lanagan *et al* [13] but only at room temperature and also without final identification of the loss mechanisms. In the system of $\text{Pb}(\text{Zr}, \text{Ti}, \text{Nb})\text{O}_3$ a strong Debye-like dielectric dispersion in the gigahertz region (also for the ceramics of these compounds) has been reported in both the paraelectric and the ferroelectric phases. The relaxation found was attributed either to sound emission by ferroelectric domain walls [14] or to the presence of clusters of micrometre or nanometre size [15].

To our knowledge there is an evident lack of experimental data on dielectric dispersion in pure *antiferroelectric* PbZrO_3 single crystal in the range of frequencies lying below that available in optical spectroscopies. Accordingly it was decided to investigate the dielectric response of this compound from 10^3 to 10^9 Hz as a function of temperature.

2. Crystal growth, sample preparation and experimental conditions

Single crystals were grown from 82.8% mol PbO –14.7% mol B_2O_3 –2.5% mol PbZrO_3 . A mixture of PbZrO_3 , PbO and B_2O_3 was placed in a Pt crucible and maintained at 1080°C for 4 h. Then the melt was cooled at rate of 8 K h^{-1} to 900°C and the solvent was poured off. Transparent light-grey crystals in the form of thin plates were obtained and revealed one phase transition from the paraelectric (cubic; $Pm3m$) to the antiferroelectric (orthorhombic, $Pbam$) phase at $T_c = 232.5^\circ\text{C}$. This direct transformation is known in the literature and has been experimentally proved by optical observation of domain structure changes and dielectric investigations [16–18].

Owing to the very good quality of as-grown crystals no polishing of surfaces was necessary. The opposite faces of sample of dimensions $2\text{ mm} \times 1\text{ mm} \times 0.06\text{ mm}$ were electroded by gold vapour deposition. Prior to making the measurements the sample was maintained at a temperature of 270°C for $\frac{1}{2}$ h in order to relieve any mechanical and electrical strain in the bulk and at the electrode–crystal interface.

The dielectric permittivity was measured with Hewlett–Packard 4191A and 4192A impedance analysers. In these layouts the sample was considered to be a lossy capacitor with lumped-circuit capacitance $C = \varepsilon' C_0$ and conductance $G = \varepsilon'' \omega C_0$ ($\omega = 2\pi f$) where C_0 and ω are the empty-cell capacitance and angular frequency, respectively. The impedance characteristic were converted directly into the real part ε' and imaginary part ε'' of the

dielectric permittivity: $\varepsilon^* = \varepsilon' - i\varepsilon''$. Investigations were performed in the frequency range $10^3 < f < 10^9$ Hz. The measuring electric field strength was equal to 17 V mm^{-1} .

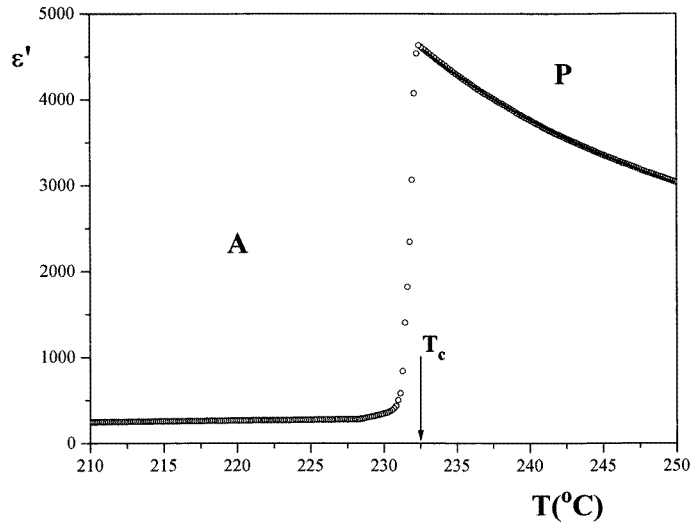


Figure 1. Temperature dependence of the real part ε' of the dielectric permittivity (10^3 Hz) in the vicinity of the phase transition from the paraelectric (P) to the antiferroelectric (A) phase in a PbZrO_3 single crystal. In the paraelectric phase the dielectric permittivity was fitted to equation (2) with $C = 1.54 \times 10^5 \pm 200$ and $T_0^* = 199.1 \pm 0.05$ (solid curve).

3. Low-frequency dielectric permittivity

Figure 1 shows typical temperature dependence of the dielectric permittivity (10^3 Hz) for the sample under investigation. The transition point T_c from the paraelectric to the antiferroelectric phase is related to the peak of the $\varepsilon'(T)$ function. The temperature dependence of ε' in the paraelectric phase ($T > T_c$) should obey the $\varepsilon'(\mathbf{k} = 0, T)$ function foreseen for the first-order antiferroelectric phase transition taking place at T_c [19, 20]:

$$\varepsilon(0, T) = \frac{1}{g + \lambda(T - T_0)} \quad (1)$$

where the constant parameters g , λ and T_0 appear in the Landau's free-energy expansion for the antiferroelectric phase and fulfil the following conditions: $g > 0$, $\lambda > 0$ and $T_0 < T_c$. Moreover g and λ are temperature-independent parameters. This relation can be rewritten in the form of the Curie–Weiss law used for ferroelectric phase transformation:

$$\varepsilon(0, T) = \frac{C}{T - T_0^*} \quad (2)$$

where $T_0^* = T_0 - g/\lambda$ and $C = 1/\lambda$.

The function (1) does not allow the experimental data for the paraelectric phase to be directly fitted since the parameters g , λ and T_0 are mutually dependent. Only the parameter λ could be calculated separately using the relation $\lambda = (1/\varepsilon_i - 1/\varepsilon_j)/(T_i - T_j)$ for both T_i and $T_j > T_c$.

Using the mathematically more convenient formula (2) the best fit of $\varepsilon'_{10^3 \text{ Hz}}(T)$ in the paraelectric phase was obtained for $T_0^* = 199.1 \pm 0.05 \text{ K}$ and $C = 1.54 \times 10^5 \pm 200 \text{ K}$ ($\lambda = 6.48 \times 10^{-6} \text{ K}^{-1}$).

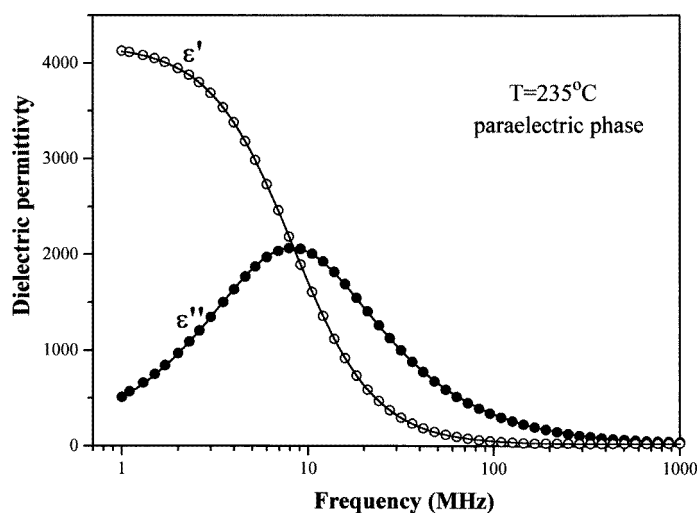


Figure 2. Example of dielectric dispersion at the chosen temperature of the paraelectric phase. The solid curves represent the fits to the Cole–Cole relation (see text).

4. High-frequency dielectric dispersion

The measurements of the dielectric dispersion in the radio-frequency range were performed in the neighbourhood of the phase transition point T_c . In figure 2 is shown an example of the recorded frequency dispersion of the real and imaginary parts of the electric permittivity in the paraelectric phase. These runs are characteristic for dipolar dispersion $\varepsilon'(f)$ and absorption $\varepsilon''(f)$ in an external field. Both exhibit a temperature dependence with increasing values of ε' especially in the low-frequency range and increasing values of ε'' which become a maximum on approaching T_c from above. The temperature evolutions of ε' and ε'' are presented in figure 3 with the maximum of ε'' shift, with decreasing temperature, towards lower frequencies. Below T_c the maximum of ε'' quickly decreases and moves to higher frequencies.

It should be stressed that this type of relaxation was observed not only in the paraelectric phase but also in the antiferroelectric phase (an example is given in figure 4). Moreover it was checked that the dispersion in the antiferroelectric phase appears in both the multiple-domain and single-domain single crystals.

The results obtained were analysed taking into account the Cole–Cole behaviour given by the complex relation

$$\varepsilon^*(\omega) = \varepsilon_{inf} + \frac{\Delta\varepsilon}{(1 + i\omega\tau)^{1-\alpha}} \quad (3)$$

where $\Delta\varepsilon$ is the dielectric step and ε_{inf} the permittivity responsible for all processes at frequencies higher than the mechanism under consideration. $\tau = f_r^{-1}$ is the mean relaxation time and ω is the angular frequency ($\omega = 2\pi f$). The parameter α is a measure

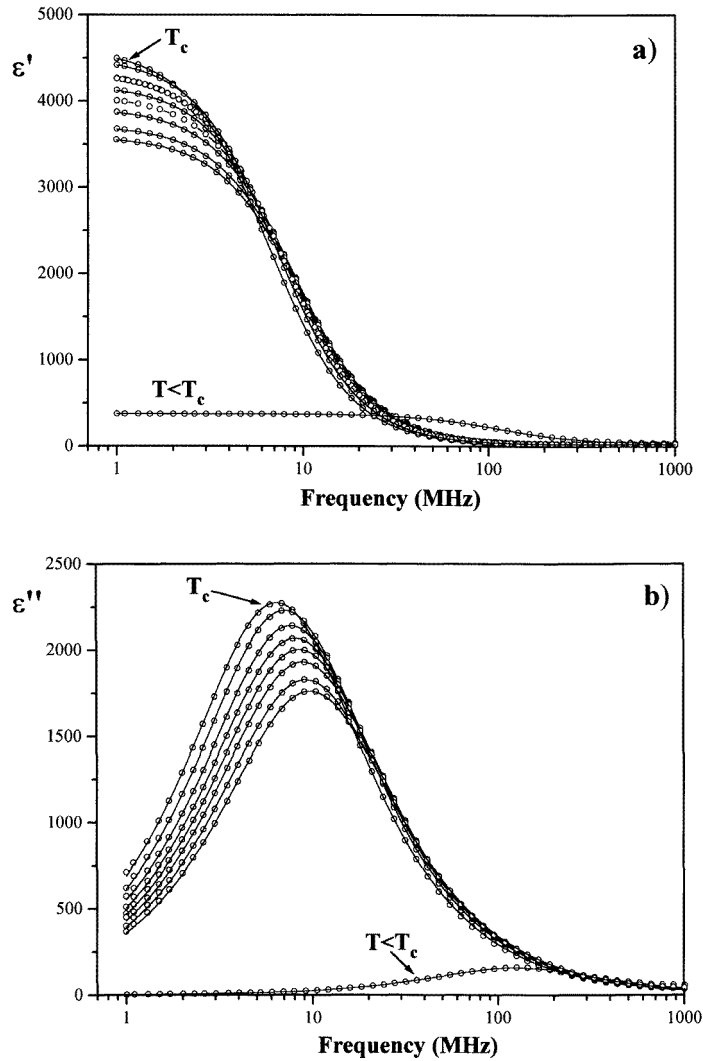


Figure 3. Temperature evolution of (a) the real part ϵ' and (b) the imaginary part ϵ'' of the dielectric permittivity. The solid curves represent fits to the Cole–Cole formula (see (3) in the text). The higher the temperature, the smaller is the ϵ' -value at 1 MHz and the smaller the maximum of $\epsilon''(f)$.

of the departure from the ideal Debye response. The $\epsilon^*(f, T)$ dependences obtained were satisfactorily fitted to the Cole–Cole relation (3) and the relaxation parameters were calculated. In the whole temperature range the parameter α is small and does not exceed the value 0.05. An increase in the value of α takes place below T_c when the antiferroelectric phase develops on cooling.

The temperature dependence of the relaxation frequency f_r is shown in figure 5(a). Attention should be paid to a distinct difference in the values of relaxation frequencies above (a few megahertz) and well below T_c (several tens of megahertz), which clearly indicates a link between the relaxation and the structural transformation taking place just in this

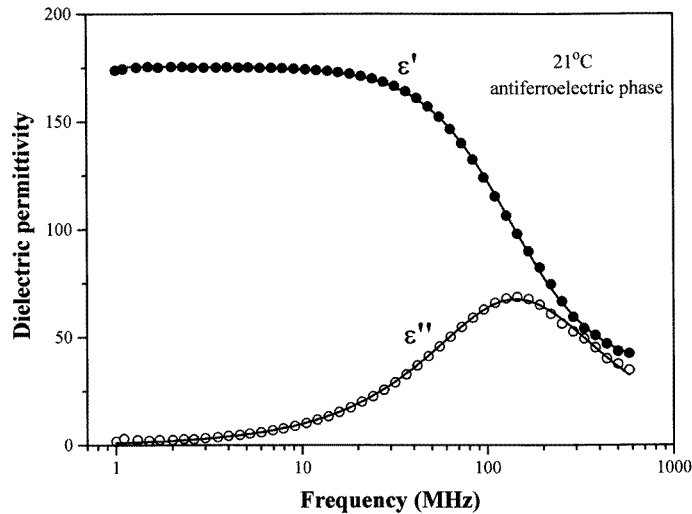


Figure 4. Frequency dependence of the real part ϵ' and the imaginary part ϵ'' of the dielectric permittivity deep in the antiferroelectric phase. Lines represent fits to the Cole–Cole formula.

temperature region. This nearly monodispersive dipolar-like relaxation which slows down at T_c may thus indicate an order–disorder mechanism of the antiferroelectric transformation in lead zirconate. However, f_r is not proportional to $T - T_0$ as has been found for a pure order–disorder phase transition, e.g. in NaNO_2 [21]. The temperature change in the relaxation frequency in the paraelectric phase is well described by the relation $f_r^2 \sim (T - T_0)$ with $T_0 = 222.9^\circ\text{C}$ (figure 5(b)). This relationship has been found to describe the dielectric relaxation in many ferroelectric BaTiO_3 -derived materials [22].

5. Share of relaxation mode in the low-frequency dielectric response

The temperature dependence of $\Delta\epsilon$ obtained from the fits of the experimental data to the Cole–Cole relation (3) is presented in figure 6 and clearly resembles the curve for the low-frequency dielectric permittivity for PbZrO_3 around T_c . It should be noted that not only the shape of $\Delta\epsilon(T)$ but also the values of the $\Delta\epsilon$ step are in good agreement with the $\epsilon'(T)$ function recorded at a frequency of 10^3 Hz (figure 1). This means that the relaxational process observed is dominant in the low-frequency dielectric behaviour within the whole temperature range investigated. The fact that in the paraelectric phase the value of the ϵ_{inf} , in which a share of lattice modes is included, is small and almost temperature independent supports this statement (see inset in figure 6).

Indeed the share of lattice phonons in the value of ϵ_{inf} can be evaluated through the Lyddane–Sachs–Teller relation. From the temperature-independent TO and LO phonon frequencies characterizing the lead perovskite crystals in the cubic phase this phonon (and electronic) share was obtained to be of the order of 30. In fact it is in good agreement with values of ϵ_{inf} . This means that the ϵ_{inf} -value obtained from the dielectric measurements corresponds to the lattice contribution and that there are no additional phenomena between the relaxational process found (10^6 – 10^9 Hz) and the lowest-frequency phonons which would have a share in the dielectric permittivity. As a consequence this relaxation process is responsible for the whole temperature behaviour of the dielectric permittivity in the cubic

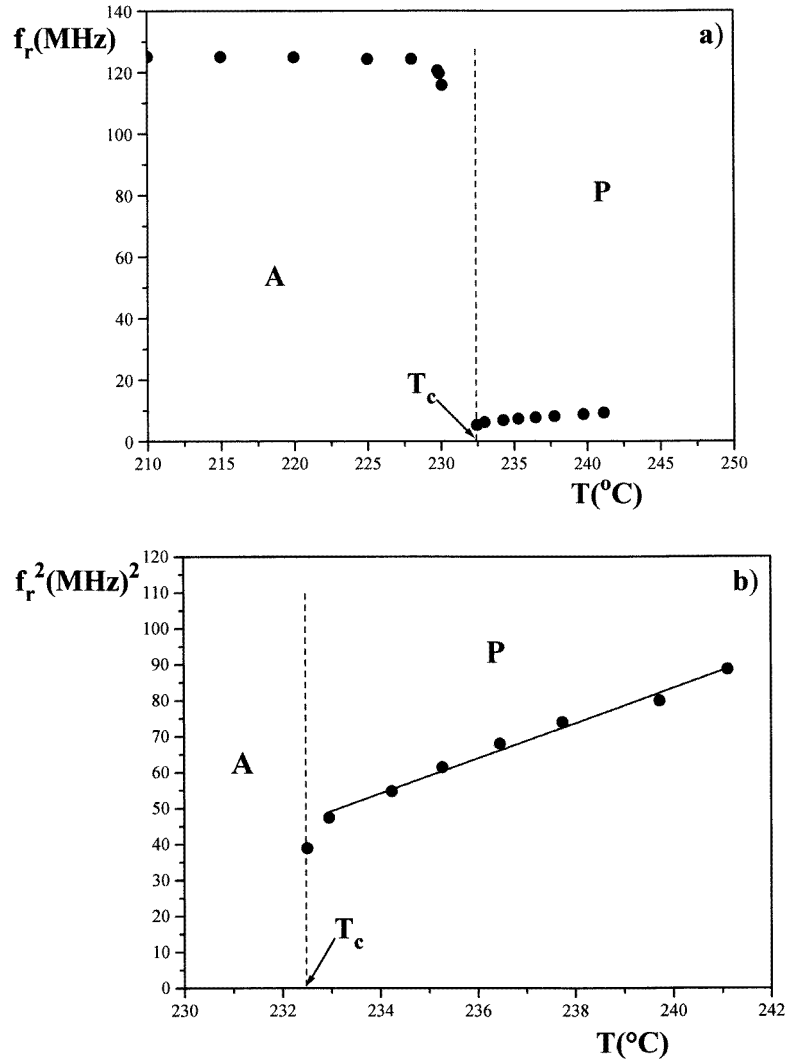


Figure 5. (a) Change in the relaxation frequency f_r during the phase transformation from the paraelectric (P) to the antiferroelectric (A) state. (b) Squared frequency in the paraelectric phase which obeys the function $f_r^2 \sim (T - T_0)$ with $T_0 = 222.9 \pm 0.1$ °C.

phase of lead zirconate.

The $\Delta\epsilon(T)$ dependence fitted to equation (2) gives $T_0^* = 201.9 \pm 0.3$ K and $C = 1.4 \times 10^5 \pm 1000$ K. The similarity of these parameters to those obtained from $\epsilon_{10^3 \text{ Hz}}(T)$ is proof of the strong link found between the relaxation and the phase transition mechanism. On the basis of this, the temperature T_0 from the relation $f_r^2 \sim (T - T_0)$ could be considered as that in equation (1) which properly describes the $\epsilon'(T)$ behaviour for the antiferroelectric phase transition. This assumption also allows the parameter g to be calculated and the parameters in equation (1) would be as follows:

$$T_0 = 222.9 \pm 0.1 \text{ °C} \quad \lambda = 6.48 \times 10^{-6} \text{ K}^{-1} \quad g = 1.55 \times 10^{-4}.$$

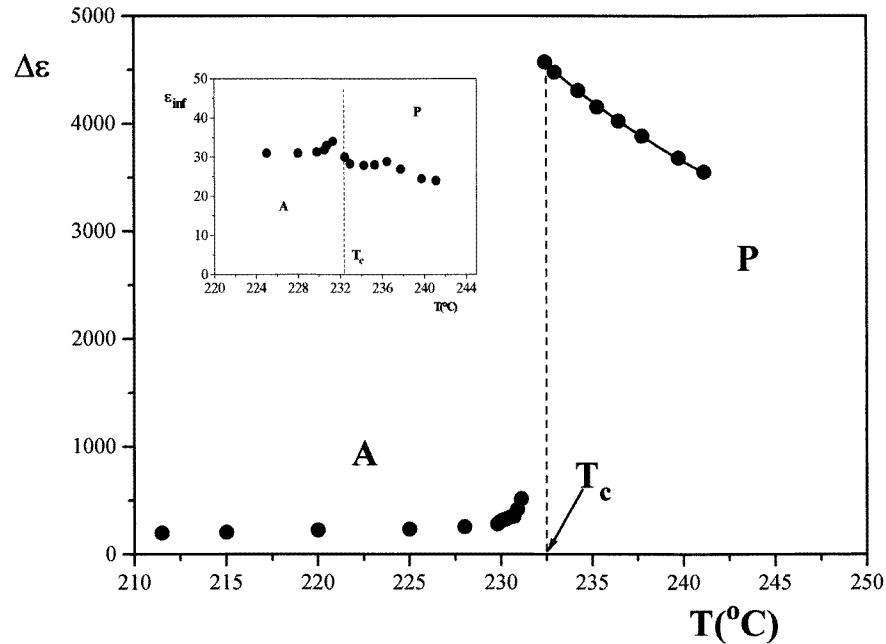


Figure 6. Dielectric step $\Delta\varepsilon$ for relaxational mode in the PbZrO_3 single crystal as a function of temperature. The solid curve represents the fit to the equation (2). The inset shows the temperature dependence of ε_{inf} around the phase transition point (see equation (3)).

6. Discussion

The measurements described above were performed on single crystals undergoing a structural phase transition directly from the cubic paraelectric to the orthorhombic antiferroelectric phase. In the literature there are reports of two kinds of PbZrO_3 sample: with and without a transient ferroelectric phase appearing just below T_c [22]. X-ray examination showed that crystals with one phase transition are structurally more perfect than those with the transient phase. The PbZrO_3 with two phase transitions exhibits structural inhomogeneity, i.e. superposition of two different orthorhombic systems, and two different cubic systems (all with nominally different lattice constants) are present in both the paraelectric and antiferroelectric phases.

The most important conclusion from this report is that in pure lead zirconate the dielectric dispersion measurements in the range from 10^6 to 10^9 Hz revealed the existence of a relaxational polar mode in the antiferroelectric and paraelectric states. This indicates the disorder–order character of the antiferroelectric phase transition in pure PbZrO_3 . The dielectric step and relaxational frequency determined from fitting the experimental data to the Cole–Cole relation showed sharp anomalies in the neighbourhood of the transition point. The temperature dependence of the dielectric step in the paraelectric phase revealed that this relaxation is almost completely responsible for the low-frequency dielectric response at T_c . Only a small departure from the Debye-type behaviour with a single relaxation time has been ascertained.

For many ABO_3 materials instead of the preponderant role of phonon softening, a nearly monodispersive dipolar relaxation was found to be responsible for the temperature

dependence of the dielectric susceptibility and its maximum at T_c . The appearance of this relaxation seems to be independent of the polar order of subsequent phases but is clearly related to the disorder–order character of the phase transitions. It should be noted that it is not limited to a specific frequency range. For instance in the solid solutions $\text{Ag}(\text{Nb}, \text{Ta})\text{O}_3$ with a variety of phase transitions an intense dipolar relaxation responsible for the temperature dependence of the static permittivity has been evidenced in the submillimetre region ($5\text{--}15\text{ cm}^{-1}$) and connected with the critical behaviour of off-centre Nb ions [24]. A monodispersive relaxation which is similar in character and which was found earlier in the range $10^6\text{--}10^9\text{ Hz}$ for BaTiO_3 and BaTiO_3 -derived materials (connected with coherent polar motion of off-centred Ti ions) seems to prove the universal behaviour of perovskite oxides at phase transitions. The far-infrared dielectric response measured for PbTiO_3 and $\text{PbZr}_x\text{Ti}_{1-x}\text{O}_3$ thin ferroelectric films [25] again showed that the existence of soft-modes does not account for the total low-frequency permittivity and indicated the existence of dielectric dispersion of several reciprocal centimetres.

The relaxation found in the *antiferroelectric* PbZrO_3 seems to support this type of behaviour. Because the relaxation frequency (especially in the paraelectric phase) is very low, it excludes a relaxation mechanism from the lattice vibrations. A model of the disorder–order phase transition related to the hopping of off-centre Zr ions between potential wells could also be applied here. However, a special role of Zr in the lead zirconate structure is to the best of our knowledge unknown in literature. Instead, the antiparallel shift of the lead ions and complex tilts of the oxygen octahedra play the main role in the antiferroelectric phase transition. The relaxation found could thus be related to disorder in the Pb or/and O sublattices.

The phase transition mechanism in ABO_3 materials containing Pb in the A position seems to be still unclear and even controversial, especially from the viewpoint of disorder in the host lattice. The temperature dependence of the nuclear quadrupole interaction at Ti sites in ferroelectric PbTiO_3 studied by perturbed angular correlation spectroscopy gave some evidence of disorder–order phenomena just in this ion site [26]. On the other hand a single-crystal neutron diffraction study of this compound gave information about distinct disorder in the Pb sublattice [27]. In particular, Pb atoms appear to be disordered at six sites displaced by about 0.2 \AA along $\langle 100 \rangle$ directions above T_c and then ordered on one of these sites below T_c . A similar phenomenon of disorder in the Pb sublattice was reported for antiferroelectric PbHfO_3 single crystals. From the Debye–Waller factor investigations in the paraelectric phase it was obtained that the Pb ions were randomly displaced; Pb can occupy one of 12 equivalent $(x, x, 0)$ positions instead of the $(0, 0, 0)$ position. From these experimental facts we incline to the opinion that in the PbZrO_3 single crystal the relaxation found could be related mainly to disorder in the Pb sublattice. Correlated motion of Pb about their displaced sites, the length of which increases on approaching T_c , may be the origin of the relaxation observed. Its low frequency and the large mass of Pb would favour this hypothesis.

Considering different origins of relaxation in the radio-frequency range it should be mentioned that well below T_c , where ϵ' is weakly temperature dependent and of the order of 200, a complex domain structure attributed to the orthorhombic symmetry might influence the dielectric response. In ferroelectric materials, domains are piezoelectrically active up to the microwave region and can emit longitudinal and shear waves into surroundings. The dielectric step related to this phenomena is of the order 10–100. On the other hand, ferroelectric domain walls can be displaced in an electric field and behave as a shear wave transducer. In this case, considerable dielectric losses may appear and relaxation is of Debye type with $\Delta\epsilon = 200\text{--}1000$. Theoretical models and experimental data can

be found in [29, 30] in which the above-mentioned phenomena directly depend on the existence of spontaneous polarization. If our sample is considered as an antiferroelectric of centrosymmetric structure below T_c , a description of the relaxation in terms of the models mentioned above does not seem to be justified. However, in view of the recently reported [31] extremely weak ferroelectricity in lead zirconate with a spontaneous polarization of $0.1 \mu\text{C cm}^{-2}$ and a local ferroelectric state occurring around the boundary of 180° domains [32], the role of these phenomena might not be negligible.

Acknowledgments

The authors thank Dr H Hassan and S Miga for discussions of and technical assistance with the measurements. This research was financially supported by the Committee for Scientific Research (KBN), Poland, under grant 2 P302 097 05.

References

- [1] Zhong W and Vanderbilt D 1995 *Phys. Rev. Lett.* **74** 2587
- [2] Zhong W, King-Smith R D and Vanderbilt D 1995 *Phys. Rev. Lett.* **72** 3618
- [3] Cochran W and Zia A 1968 *Phys. Status Solidi* **25** 273
- [4] Fujishita H and Hoshino S 1984 *J. Phys. Soc. Japan* **53** 226
- [5] Singh D J 1995 *Phys. Rev. B* **52** 12 559
- [6] Glazer A M, Roleder K and Dec J 1993 *Acta Crystallogr. B* **49** 846
- [7] Pasto A E and Condrate R E 1973 *J. Am. Ceram. Soc.* **56** 436
- [8] Roleder K, Kugel G E, Hańderek J, Fontana M D, Carabatos C and Kania A 1988 *Ferroelectrics* **80** 809
- [9] Laabidi K, Fontana M D, Maglione M, Jannot B and Muller K A 1994 *Europhys. Lett.* **26** 309
- [10] Sokoloff J P, Chase L L and Rytz D 1998 *Phys. Rev. B* **38** 597
- [11] Fontana M D, Idrissi M and Wójcik K 1990 *Europhys. Lett.* **11** 419
- [12] Maglione M, Bohmer R, Loidl A and Hochli U T 1989 *Phys. Rev. B* **40** 11 441
- [13] Lanagan M T, Kim J H, Sei-Jeo Jang and Newnham R E 1988 *J. Am. Ceram. Soc.* **71** 311
- [14] Arlt G, Bottger U and Witte S 1994 *Ann. Physik Lpz.* **3** 578
- [15] Hassan H, Maglione M, Fontana M D and Hańderek J 1995 *J. Phys.: Condens. Matter* **7** 8647
- [16] Samara G A 1970 *Phys. Rev. B* **1** 3777
- [17] Dec J and Kwapuliński J 1989 *J. Phys.: Condens. Matter* **1** 3389
- [18] Roleder K and Dec J 1989 *J. Phys.: Condens. Matter* **1** 1503
- [19] Okada K 1969 *J. Phys. Soc. Japan* **27** 420
- [20] Okada K 1970 *J. Phys. Soc. Japan Suppl.* **28** 420
- [21] Hatta M I 1968 *J. Phys. Soc. Japan* **24** 1034
- [22] Kazaoui S, Ravez J, Elissalde L and Maglione M 1992 *Ferroelectrics* **125** 85
- [23] Dec J and Kwapuliński J 1989 *Phase Trans.* **18** 1
- [24] Volkov A A, Gorshunov B P, Komandin G, Fortin W, Kugel G E, Kania A and Grigas J 1995 *J. Phys.: Condens. Matter* **7** 785
- [25] Fedorov I, Petzelt J, Zelezny V, Komandin G A, Volkov A A, Brooks K, Huang Y and Setter N 1995 *J. Phys.: Condens. Matter* **7** 4313
- [26] Catchen G L, Wukitch S J, Spaar D M and Blaszkiewicz M 1990 *Phys. Rev. B* **42** 1885
- [27] Nelmes J, Piltz R O, Kuhs W F, Tun Z and Restori R 1990 *Ferroelectrics* **108** 165
- [28] Kwapuliński J, Pawelczyk M and Dec J 1994 *J. Phys.: Condens. Matter* **6** 4655
- [29] Pertsev N A and Arlt G 1993 *J. Appl. Phys.* **7** 4105
- [30] Arlt G, Bottger V and Witte S 1994 *J. Am. Ceram. Soc.* **78** 1
- [31] Dai X, Li J F and Viehland D 1995 *Phys. Rev. B* **51** 2651
- [32] Tanaka M, Saito R and Tsuzuki K 1982 *Japan. J. Appl. Phys.* **21** 291